Eng. Sci., 2022, **17**, 83–90

Engineered Science

DOI: https://dx.doi.org/10.30919/es8d570

Highly Isolated Ultrawideband Multiple Input and Multiple Output Antenna for Wireless Applications

Praveen Kumar,[1] Tanweer Ali[1,*] and Manohara Pai M. M.[2]

Abstract

The paper presents, a compact planar two-element ultrawideband (UWB) multiple-input, and multiple-output (MIMO) antenna. The work constitutes a half-circle shape radiating and lowered ground plane monopole antenna. The total area of the UWB MIMO antenna is 13.5 × 30 × 1.6 mm^3. The proposed structure has an impedance bandwidth of 150% (1.6 - 11.4 GHz) in simulation and about 145% (1.8 - 11.3 GHz) in measurement and average isolation better than 30 dB in the UWB range. Various diversity parameters are also evaluated as described below. Envelope correlation coefficient (ECC) is less than 0.001, diversity gain (DG) is more than 9.9, mean effective gain (MEG) is below - 6 dB, channel capacity loss (CCL) is less than 0.2 bps/Hz, total active reflection coefficient (TARC) less than -10 dB, and multiplexing efficiency less than zero over an operating frequency band. The time-domain analysis is carried out, particularly group delay and fidelity factor. The results of time-domain analysis guarantee that the output pulses are less sensitive to interference.

Keywords: Ultrawideband (UWB) antenna; Compact, Multiple-input, and multiple-output (MIMO) antenna; Diversity parameters.
Received: 12 October 2021; Revised: 02 November 2021; Accepted: 11 November 2021.
Article type: Research article.

1. Introduction

The advancement in technologies such as the internet of things and its applications, global positioning systems, cellular communication, *etc*., greatly relies on wireless communication. In recent years, modern wireless communication systems witnessed many new technologies that make communication systems more reliable. Simultaneously the data traffic increases exponentially day by day, demanding high data rate, compact size, and security.[1] To meet this requirement, two promising technologies are evolved (1) ultrawideband (UWB), (2) multiple-input, and multiple-output (MIMO). The UWB technology offers an unlicensed bandwidth of 7.5 GHz for short-range wireless communication applications in the range from 3.1 - 10.6 GHz allotted by the federal communication commission (FCC).[2] The power radiation in UWB is regulated to below -41.3 dBm/MHz. This technology provides a large bandwidth and hence increases channel capacity. However, the confinement of effective isotropic radiated power (EIRP) results in an aggravating problem of multipath and channel fading. Communication systems require a technology that uses multipath fading in favorable scenarios rather than mitigation to overcome this problem. One such technology is MIMO. Therefore, the integration of UWB and MIMO provides increased link reliability.

The increase in channel capacity in UWB MIMO is by placing more antennas at the transmitter and receiver. But the incorporation of multiple antennas in a compact size (like mobile communication) introduces strong interference amongst the antenna elements known as mutual coupling. Hence, it is necessary to have strong isolation among the antenna element in UWB MIMO to achieve an increased channel capacity.

Several studies have been conducted over the last decades to increase the isolations or reduce the mutual coupling among the elements of UWB MIMO antennas. Broadly all techniques are classified into two ways: suppressing the mutual coupling and providing an alternate current path. Orthogonal placement of antennas results in high isolation between the antenna elements.[3-5] This technique holds good for the design where antenna dimensions are not a severe constraint. Modifying the ground plane by engraving slits, and slots, and introducing stubs increases the isolation amongst the element by

[1] *Department of Electronics and Communication, Manipal Institute of Technology, Manipal Academy of Higher Education, Manipal 576104, India.*

[2] *Department of Information and Communication Technology, Manipal Institute of Technology, Manipal Academy of Higher Education, Manipal 576104, India.*

* *E-mail:* tanweer.ali@manipal.edu (T. Ali)

disturbing the surface current distribution.[6-15] The shape of parasitic elements such as slits, slots, and stubs is vital because the structures are frequency-dependent. Decoupling between the MIMO antenna is accomplished by providing the additional matching network that mitigates the mutual impedance among the antenna elements.[16] The metamaterial elements in a MIMO antenna system disrupt the current distribution and decouples between neighboring antenna components. Metamaterial structures resonant behavior limits the magnetic field well within the stimulated antenna, suppressing mutual coupling. The literature unveils different approaches to metamaterial utilization onto radiating and ground planes of the MIMO antenna system. The loading of metamaterial shapes such as split-ring resonators and their variants engrosses the coupling effect between the elements.[17-19] The array of metamaterial structures are commonly referred to as metasurface. The metasurface loading into the antenna structure like electromagnetic bandgap,[20,21] frequency selective surface,[22,23] and composite right and left-hand unit cell[24] behaves as band stop filter and leads to suppression of mutual coupling. The stimulation of different orthogonal characteristic modes suppresses the coupling effect and results in a very low correlation.[25] The techniques mentioned above belong to the category of suppressing the coupling effect. The neutralization line[26-28] technique delivers reduced mutual coupling by providing alternate current paths. A combination of any aforementioned methods can also be utilized for improving isolation in MIMO antennas.[29] This paper proposes a two-element MIMO antenna consisting of a half-circle shape UWB monopole antenna with an impedance bandwidth of 145% (1.8 - 11.3 GHz). For enhancement of isolation[30] is considered as a reference and lowered ground plane and spiral stub help in achieving good isolation. The proposed antenna structure exhibit isolation better than 30 dB over operating bandwidth. MIMO diversity parameters are evaluated for the effectiveness of the design and suitability for MIMO applications.

2. Antenna design

The proposed UWB MIMO antenna is modeled on Flame Retardant 4 (FR-4) substrate with a dimension of 13.5 × 30 × 1.6 mm^3, as depicted in Fig. 1. FR-4 is glass-reinforced epoxy laminate material having the properties of electric permittivity of 4.4, the dielectric loss tangent of 0.02, and thickness of 1.6 mm. This configuration has two elements placed side by side with a separation of 9.2 mm. A 50 Ω microstrip line feeds the antennas. The antenna element is made up of a half-circle shape monopole patch, the common lowered ground plane having a spiral stub. The appropriate selection of the half-circle patch length helps achieve impedance bandwidth in the UWB range. The stub on the ground plane terminates the maximum coupling current and creates a local path. This change in surface current distribution results in improved isolation.

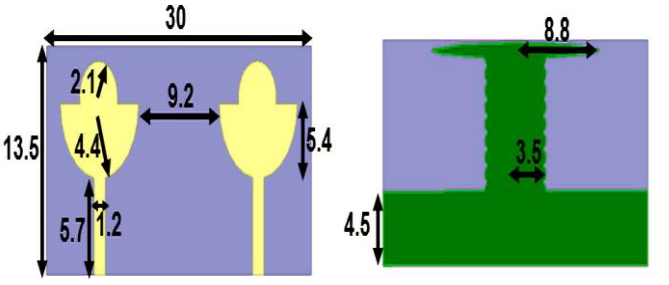

Fig. 1 Two-element UWB MIMO structure (dimensions in mm).

The surface current distribution of the proposed antenna configuration at frequencies 3.15 GHz and 8.52 GHz are depicted in Fig. 2. Current distribution is examined by stimulating one port and terminating the other port for matched conditions. The maximum current is at the feedline of the patch and is limited to the stub and ground plane. The adjacent element has negligible current influence from the stimulated antenna element as illustrated in Fig 2. This confirms that the addition of stubs on the ground plane improves the isolation of the MIMO antenna elements.

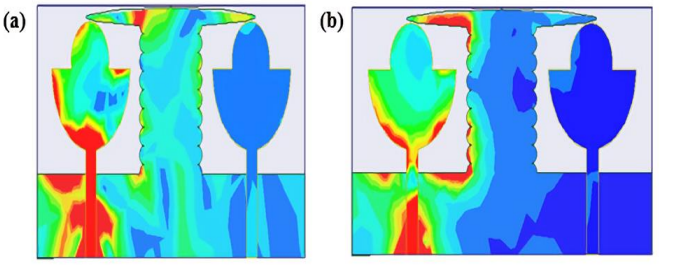

Fig. 2 Current distribution of UWB MIMO by terminating port 2 at (a) 3.15 GHz, (b) 8.52 GHz.

3. Results and discussion

The proposed antenna configuration is simulated in high-frequency structure simulator (HFSS) software based on a finite element method solver from analysis of systems (ANSYS). Various parameters are studied, such as S-parameters, radiation patterns, and diversity parameters, to assess the effectiveness of the design. The prototype of the proposed design is depicted in Fig. 3.

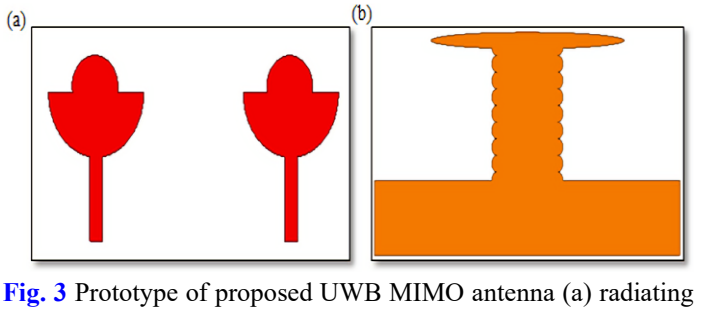

Fig. 3 Prototype of proposed UWB MIMO antenna (a) radiating plane (b) ground plane.

3.1 S-parameters and Radiation pattern

The S-parameters of the proposed antenna structure are depicted in Fig. 4. It has an impedance bandwidth ranging from 1.6-11.4 GHz in simulation and about 1.8-11.3 GHz

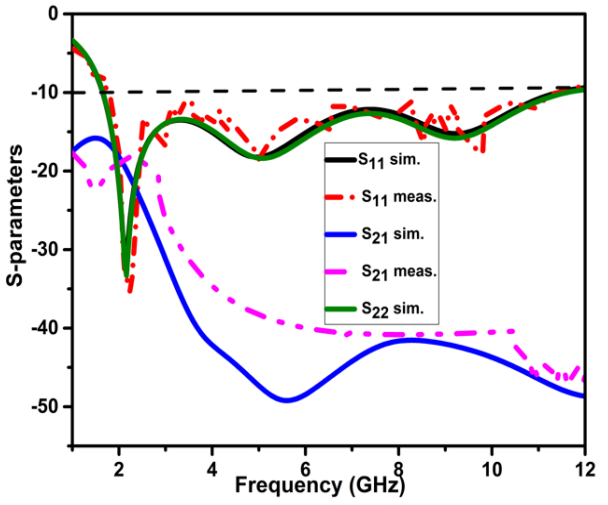

Fig. 4 Simulated and measured S-parameters of the proposed UWB MIMO antenna.

under measurement, thus, covering the UWB range. The decoupling structure at the ground plane provides isolation below 30 dB in the UWB range. Validation of simulated results is performed by fabricating the proposed design on an FR-4 substrate.

Equations 1 and 2 depict reflection (S_{11}/S_{22}) and transmission coefficients (S_{12}/S_{21}) using source impedance (Z_S) and load impedance (Z_L).

$$Reflection\ coefficient\ =\ \frac{Z_L - Z_S}{Z_L + Z_S} \quad (1)$$

$$Transmission\ coefficient\ =\ \frac{2Z_L}{Z_L + Z_s} \quad (2)$$

The radiation pattern can be represented as a graphical representation of received power as a function of a spherical coordinate system, as in equation 3. The radiation intensity for far-field is:

$$U\ =\ r^2\, W_{rad}\ =\ B_0\, F(\theta,\phi)\ =\simeq \frac{r^2}{\eta}\left[|E_\theta(r,\theta,\phi)|^2 + \left|E_\phi(r,\theta,\phi)\right|^2\right] \quad (3)$$

where U radiation intensity (W/unit solid angle), W_{rad} radiation density (W/m^2), $E(r,\theta,\phi)$ far zone electric field intensity of the antenna, E_θ, E_ϕ far zone electric field components of antenna, η intrinsic impedance of the medium. The radiation pattern of the proposed UWB MIMO structure for the frequencies 3.15 GHz and 8.52 GHz is shown in Fig. 5. The figure describes for ϕ-polarized elements (0 and 90 degrees) in the two principal planes E and H are nearly bidirectional and omnidirectional pattern.

3.2 Diversity Parameters

Various diversity parameters are evaluated using S-parameters to determine the efficacy of the proposed antenna configuration as follows. The envelope correlation coefficient (ECC) is less than 0.001and diversity gain (DG) is greater than 9.9 over impedance bandwidth as depicted in Fig. 6a. The mean effective gain (MEG between port 1 and 2) is less than -6 dB, and channel capacity loss (CCL) is less than 0.2 bps/Hz as shown in Fig. 6b. The aforementioned diversity parameters are calculated using S-parameter as follows[31-34]:

The correlation coefficient is given by equation 4,

$$\rho_{ij}\ =\ \frac{-\sum_{n=1}^{N} S_{ni}^{*}\, S_{nj}}{\sqrt{\left(1-\sum_{n=1}^{N}|S_{ni}|^2\right)\left(1-\sum_{n=1}^{N}|S_{nj}|^2\right)}} \quad (4)$$

ECC is defined as the square of the correlation coefficient, and for a two-element MIMO antenna, ECC is described in equation 5.

$$ECC\ =\ \frac{|S_{11}^{*}\, S_{12} + S_{21}^{*}\, S_{22}|^2}{(1-|S_{11}|^2-|S_{21}|^2)(1-|S_{22}|^2-|S_{12}|^2)} \quad (5)$$

Equations 6-8 are used for calculating DG, MEG, and CCL for projected antenna design:

$$DG\ =\ 10\sqrt{1-ECC^2} \quad (6)$$

$$MEG_i\ =\ 0.5\left(1-\sum_{j=1}^{M}|S_{ij}|\right) \quad (7)$$

$$CCL\ =\ -log_2 \det(\alpha)^R \quad (8)$$

where α^R is the receiving antenna correlation matrix for two-element α^R is as follows:

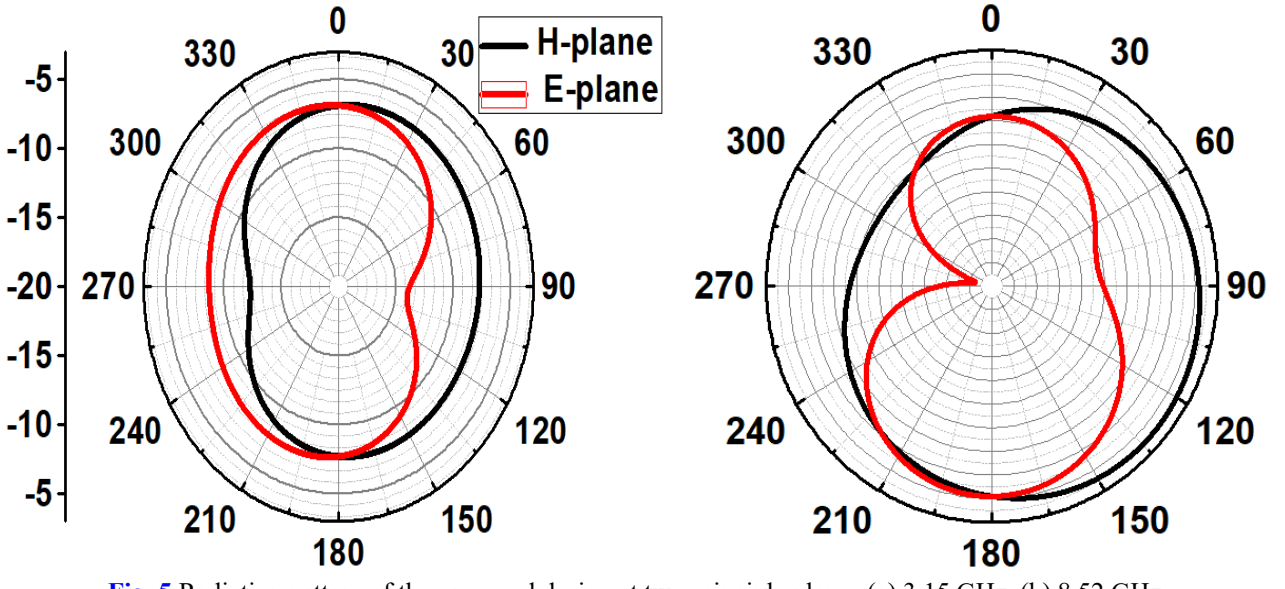

Fig. 5 Radiation pattern of the proposed design at two principle planes (a) 3.15 GHz, (b) 8.52 GHz.

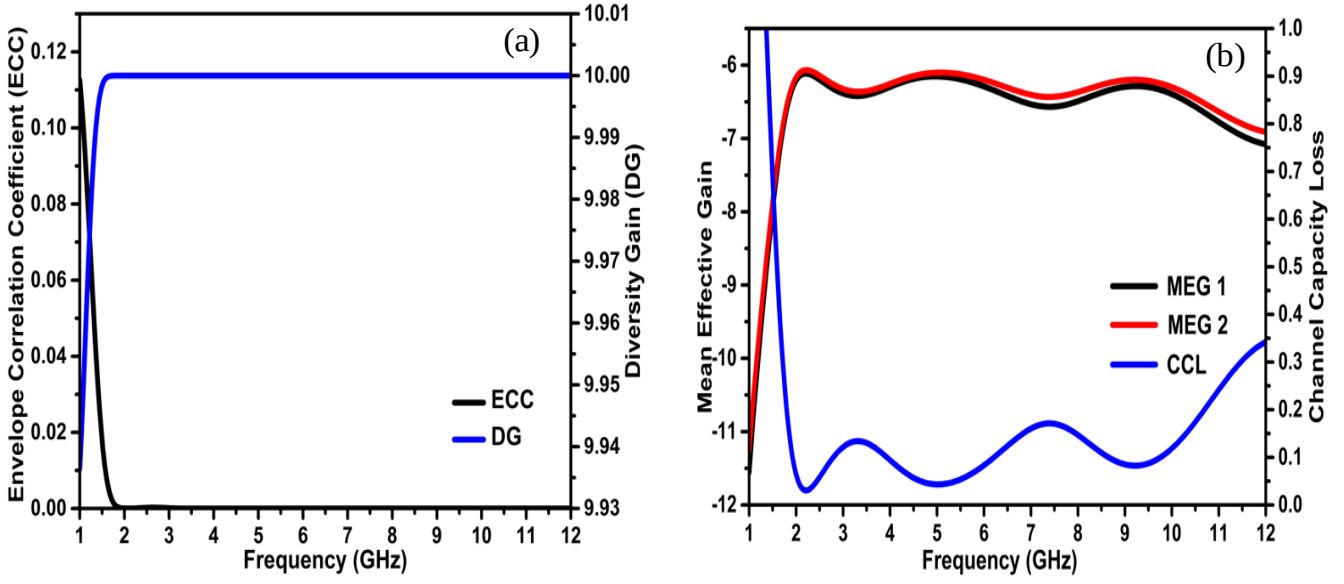

Fig. 6 MIMO Diversity parameters of UWB MIMO (a) envelope correlation coefficient (ECC) and diversity gain (DG) (b) mean effective gain (MEG) and channel capacity loss (CCL).

$\alpha^R = \begin{vmatrix} \rho_{11} & \rho_{12} \\ \rho_{21} & \rho_{22} \end{vmatrix}$,

where $\rho_{ii} = 1 - \left|\sum_{n=1}^{N=2} S_{i,n}^* S_{n,i}\right|$ and $\rho_{ij} = -\left|\sum_{n=1}^{N=2} S_{i,n}^* S_{n,j}\right|$, For $i, j = 1, 2$.

The variation in the power needed for a MIMO antenna (under test) to attain a certain capacity in contrast to the ideal standard MIMO antenna is defined as multiplexing efficiency (ME). In addition to the above-mentioned diversity parameters, the total active reflection coefficient (TARC) provides effective operating bandwidth of the MIMO antenna by considering the coupling and random signal combination. The TARC and ME of the proposed design are well below the -10 dB and less than -1 dB over impedance bandwidth as depicted in Figs. 7a and 7b, respectively. These values illustrate that the proposed antenna configuration is well-suitable for MIMO applications. The value of TARC and ME are calculated using S-parameters, as shown in equations 9 and 10.

$$TARC = \sqrt{\frac{(S_{11}+S_{12})^2+(S_{21}+S_{22})^2}{2}} \quad (9)$$

$$ME = \sqrt{\eta_i \eta_j (1 - |\rho_{ij}|^2)} \quad (10)$$

where η_i, η_j are total efficiency of i[th] and j[th] element, ρ_{ij} is the correlation coefficient between the i[th] and j[th] element.

3.3 Time-domain analysis

The specifications defined by the federal communication commission (FCC) for designing ultrawideband (UWB) antennas require additional design parameters other than the normal antennas. The UWB offers an unlicensed 7.5 GHz frequency band between 3.1 to 10.6 GHz for short-range communication. For this purpose, UWB uses short pulses for transmitting and receiving signals. In this process, there is a chance of getting signal distortion and dispersion because of the communication path and distance. Additional parameters analysis is required to quantify this effect, such as group delay, fidelity factor, and isolation, to ensure that transmitted and received signals are in phase.[35]

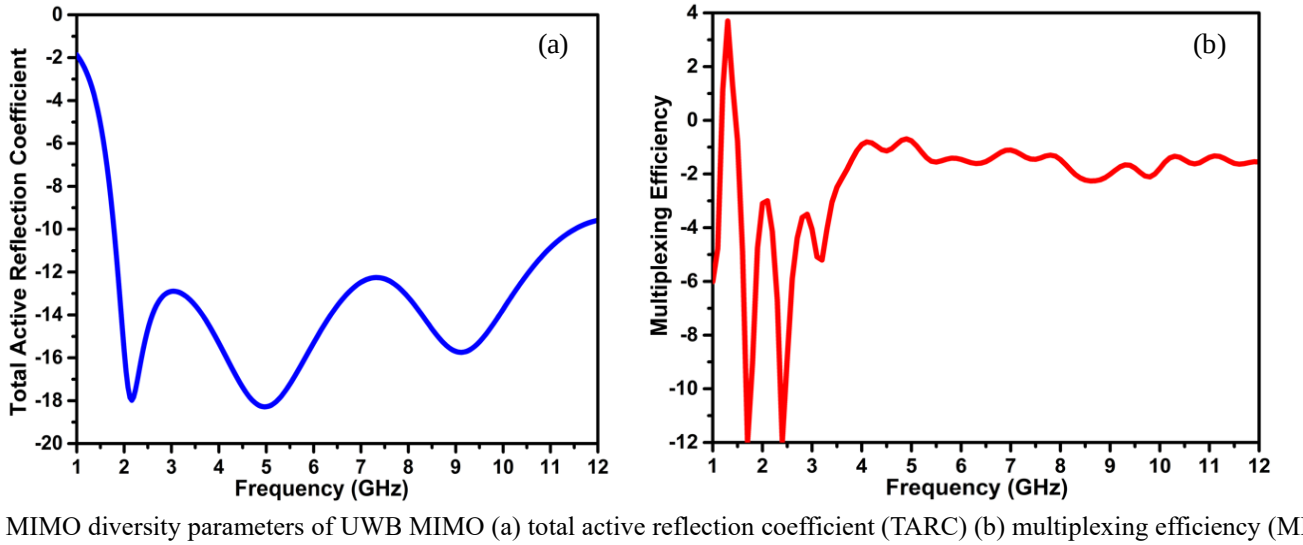

Fig. 7 MIMO diversity parameters of UWB MIMO (a) total active reflection coefficient (TARC) (b) multiplexing efficiency (ME).

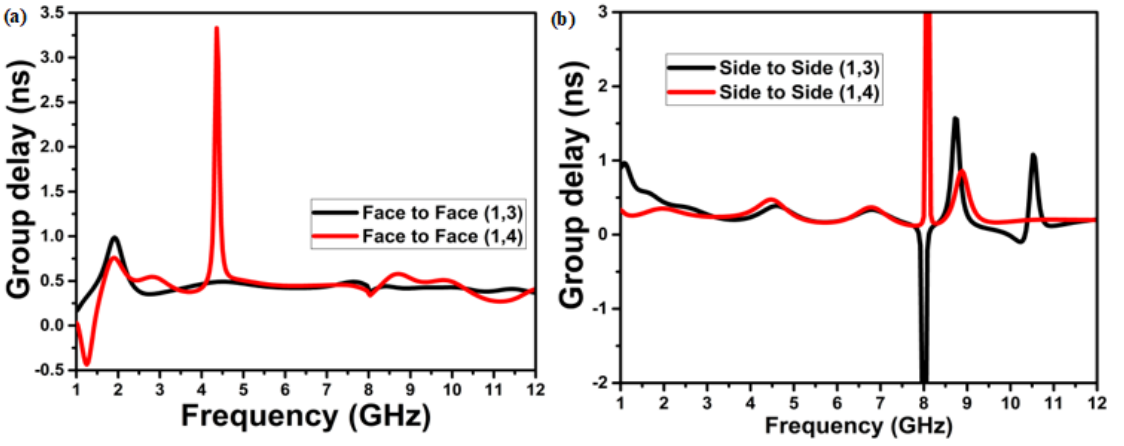

Fig. 8 Group delay of the proposed antenna design (a) face-to-face (b) side-to-side orientation.

To analyze the above-mentioned parameters, two identical designed antennas, *i.e.*, face-to-face and/or side-to-side orientation, are placed at a 100 mm distance. So that transmitted and received pulse properties can be examined for smooth communication. To evaluate the linear phase between transmitted and received pulses, group delay ($\tau_g(\omega)$) or time delay of the system is used. The group delay is a derivative of the phase response of the system with respect to the angular frequency. The fidelity factor (FF) examines the transmitted and received pulse shape and not amplitude of the pulses. It gives information about pulse distortion. The group delay and FF can be evaluated using the following equations 11 and 14,

$$\tau_g(\omega) = -\frac{d\varphi(\omega)}{d\omega} \quad (11)$$

where φ is the phase between the ports.

To evaluate FF, normalized transmitted (T_s^n) and received a pulse (R_s^n) is evaluated by equations 12 and 13, respectively.

$$T_s^n = \frac{T_s(t)}{\sqrt{\int_{-\infty}^{\infty}|T_s(t)|^2 dt}} \quad (12)$$

$$R_s^n = \frac{R_s(t)}{\sqrt{\int_{-\infty}^{\infty}|R_s(t)|^2 dt}} \quad (13)$$

$$FF = \max \int_{-\infty}^{\infty} T_s^n(t)\ R_s^n(t+\tau)\, dt \quad (14)$$

The group delay of the proposed design for side-to-side and face-to-face orientation is depicted in Fig. 8. It can be observed that the group delay is less than 1 ns except for some frequency over impedance bandwidth.

A side-to-side and face-to-face orientation is used for calculating the fidelity factor. The input and output signals are normalized, as depicted in Fig. 9. Normalization is used to guarantee that just the structure of the signals is evaluated rather than their amplitude. The similarity between the transmitted and received pulses is calculated using the earlier equations' fidelity factor and listed in Table 1. The calculated fidelity factor values ensure that the pulse received at the receiver has a more negligible effect of interference.

Table 1. Fidelity factor for different orientations and ports.

Orientation	Ports	Fidelity factor
Side to Side	1 and 3	99.62
	1 and 4	99
Face to Face	1 and 3	98.73
	1 and 4	99.13

4. Performance comparison

Table 2 summarizes the performance of antennas from various

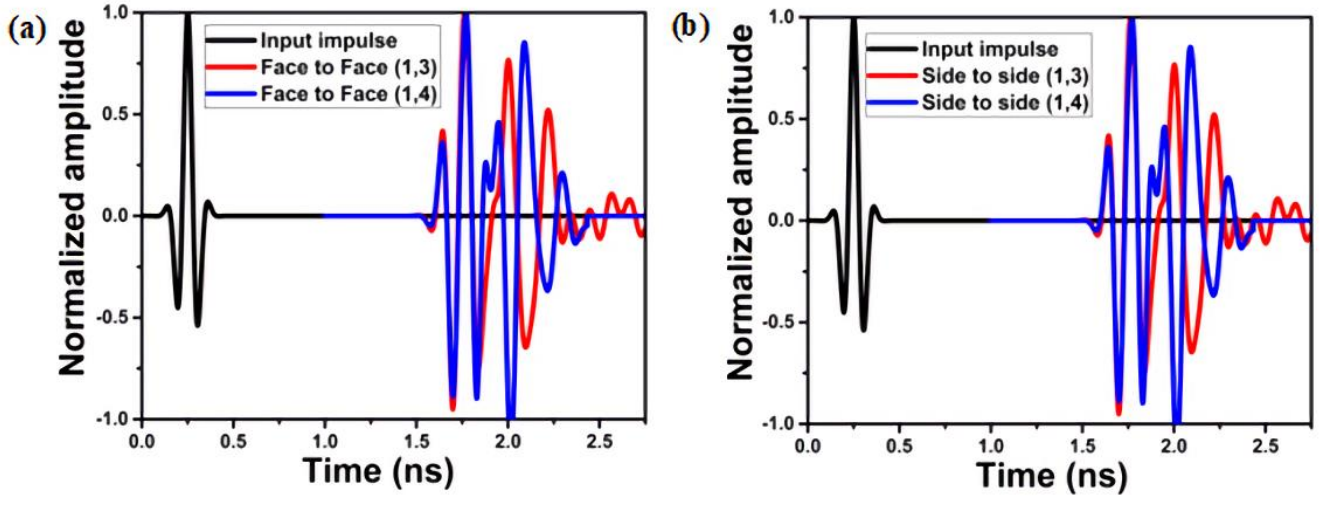

Fig. 9 Normalized amplitude of input and output pulses (a) face to face (b) side to side.

Table 2. Comparison analysis with existing literature designs.

Reference	Dimension (mm^2)	Bandwidth (GHz)	Isolation (dB)	Diversity parameters						$\tau_g(\omega)$ (ns)	FF (%)
				A	B	C	D	E	F		
J. Tao *et al.*[9]	18×34	2.93-20	<-22	<0.01	>9.95	<1	<-20	-	<0	-	-
L. Y. Nie *et al.*[10]	120×110	3-10	<-38	<0.0002	-	-	-	-	-	-	-
L. Y. Nie *et al.*[11]	50×60	2.98-10	<-31.4	<0.5	≈10	-	-	-	-	-	-
L. Wang *et al.*[12]	35×50	3-11	<-25	<0.004	-	-	-	-	-	-	-
M. Agarwal *et al.*[13]	35×46	2.1-11.4	<-24.5	<0.04	≈10	-	-	-	-	-	-
S. Luo *et al.*[14]	39×30	3-11	<-20	<0.02	>9.8	-	<-5.7	-	-	-	-
A. H. Jabire *et al.*[19]	43×34.9	3-10.7	<-25	0.01	≈10	-	-	-	-	-	-
J. Zhu *et al.*[36]	35×35	3-12	<-20	<0.3	-	<-3	-	-	-	-	-
J. Y. Deng *et al.*[7]	30×40	3.1-10.6	<-15	<0.15	-	-	-	-	-	<1	-
A. Iqbal *et al.*[37]	50×30	2.5-14.5	<-20	<0.04	>7.4	-	-	-	<-.5	-	-
G. Srivastava *et al.*[38]	36×18	3.2-12	<-22	<0.01	-	-	-	<0.4	-	-	-
This Work	13.5×30	1.6-11.4	<-30	<0.01	>9.9	<-6	<-10	0.2	<0	<1	99

*- not available, A-ECC, B-DG, C-MEG, D-TARC (dB), E-CCL (bps/Hz), F-ME (dB)

literature to emphasize the merits of the presented MIMO antenna. The presented antenna has wide bandwidth with good isolation and diversity parameters.

5. Conclusions

This communication presents a compact two-element MIMO antenna operating in the UWB range. The stub on the ground plane assists in achieving isolation stronger than 30 dB in the UWB spectrum. The diversity parameters ECC, DG, MEG, CCL, TARC, and ME have been analyzed to examine the effectiveness of the proposed antenna configuration. These results confirmed that the MIMO antenna proposed is appropriate for wireless UWB applications. Time-domain analysis (group delay and fidelity factor) is also performed on the proposed MIMO antenna design, and its results confirm that the output pulses are less exposed to inter-symbol interference.

Conflict of interest

There are no conflicts to declare.

Supporting information

Not applicable.

References

[1] R. Chataut, R. Akl, Massive MIMO systems for 5G and beyond networks—overview, recent trends, challenges, and future research direction, *Sensors*, 2020, **20**, 2753, doi: 10.3390/s20102753.

[2] "Ultra-wideband operations FCC report and order," Tech. Rep. (US 47 CFR part 15, 2002).

[3] L. Liu, S. W. Cheung, T. I. Yuk, Compact MIMO antenna for portable devices in UWB Applications, *IEEE Transactions on Antennas and Propagation*, 2013, **61**, 4257-4264, doi: 10.1109/TAP.2013.2263277.

[4] M. G. N. Alsath, M. Kanagasabai, Compact UWB monopole antenna for automotive communications, *IEEE Transactions on Antennas and Propagation*, 2015, **63**, 4204-4208, doi: 10.1109/tap.2015.2447006.

[5] Z. Tang, X. Wu, J. Zhan, S. Hu, Z. Xi, Y. Liu, Compact UWB-MIMO antenna with high isolation and triple band-notched characteristics, *IEEE Access*, 2019, **7**, 19856-19865, doi: 10.1109/access.2019.2897170.

[6] C. M. Luo, J. S. Hong, L. L. Zhong, Isolation enhancement of a very compact UWB-MIMO slot antenna with two defected ground structures, *IEEE Antennas and Wireless Propagation Letters*, 2015, **14**, 1766-1769, doi: 10.1109/lawp.2015.2423318.

[7] J. Y. Deng, L. X. Guo, X. L. Liu, An ultrawideband MIMO antenna with a high isolation, *IEEE Antennas and Wireless Propagation Letters*, 2016, **15**, 182-185, doi: 10.1109/lawp.2015.2437713.

[8] J. Tao, Q. Feng, Compact Ultrawideband MIMO Antenna With Half-Slot Structure, *IEEE Antennas and Wireless Propagation Letters*, 2016, **16**, 792-795, doi: 10.1109/LAWP.2016.2604344.

[9] R. Chandel, A. K. Gautam, K. Rambabu, Tapered fed compact UWB MIMO-diversity antenna with dual band-notched characteristics, *IEEE Transactions on Antennas and Propagation*, 2018, **66**, 1677-1684, doi: 10.1109/tap.2018.2803134.

[10] L. Y. Nie, X. Q. Lin, Z. Q. Yang, J. Zhang, B. Wang, Structure-shared planar UWB MIMO antenna with high isolation for mobile platform, *IEEE Transactions on Antennas and*

Propagation, 2019, **67**, 2735-2738, doi: 10.1109/tap.2018.2889596.
[11] L. Y. Nie, X. Q. Lin, S. Xiang, B. Wang, L. Xiao, J. Y. Ye, High-isolation two-port UWB antenna based on shared structure, *IEEE Transactions on Antennas and Propagation*, 2020, **68**, 8186-8191, doi: 10.1109/tap.2020.2997461.
[12] L. Wang, Z. Du, H. Yang, R. Ma, Y. Zhao, X. Cui, X. Xi, Compact UWB MIMO antenna with high isolation using fence-type decoupling structure, *IEEE Antennas and Wireless Propagation Letters*, 2019, **18**, 1641-1645, doi: 10.1109/lawp.2019.2925857.
[13] M. Agarwal, J. K. Dhanoa, M. K. Khandelwal, Two-port hexagon shaped MIMO microstrip antenna for UWB applications integrated with double stop bands for WiMax and WLAN, *AEU - International Journal of Electronics and Communications*, 2021, **138**, 153885, doi: 10.1016/j.aeue.2021.153885.
[14] S. Luo, D. Wang, Y. Chen, E. Li, C. Jiang, A compact dual-port UWB-MIMO antenna with quadruple band-notched characteristics, *AEU - International Journal of Electronics and Communications*, 2021, **136**, 153770-153779, doi: 10.1016/j.aeue.2021.153770.
[15] D. Sipal, M. P. Abegaonkar, S. K. Koul, Easily extendable compact planar UWB MIMO antenna array, *IEEE Antennas and Wireless Propagation Letters*, 2017, **16**, 2328-2331, doi: 10.1109/lawp.2017.2717496.
[16] K.-D. Xu, H. Luyen, N. Behdad, A decoupling and matching network design for single- and dual-band two-element antenna arrays, *IEEE Transactions on Microwave Theory and Techniques*, 2020, **68**, 3986-3999, doi: 10.1109/tmtt.2020.2989120.
[17] G. Zhai, Z. N. Chen, X. Qing, Enhanced Isolation of a Closely Spaced Four-Element MIMO Antenna System Using Metamaterial Mushroom, *IEEE Transactions on Antennas and Propagation*, 2015, **63**, 3362-3370, doi: 10.1109/TAP.2015.2434403.
[18] V. Najafy, M. Bemani, Mutual-coupling reduction in triple-band MIMO antennas for WLAN using CSRRs, *International Journal of Microwave and Wireless Technologies*, 2020, **12**, 762-768, doi: 10.1017/S1759078720000215.
[19] A. H. Jabire, A. Ghaffar, X. J. Li, A. Abdu, S. Saminu, M. Alibakhshikenari, F. Falcone, E. Limiti, Metamaterial based design of compact UWB/MIMO monopoles antenna with characteristic mode analysis, *Applied Sciences*, 2021, **11**, 1542, doi: 10.3390/app11041542.
[20] X. Tan, W. Wang, Y. Wu, Y. Liu, A. A. Kishk, Enhancing isolation in dual-band meander-line multiple antenna by employing split EBG structure, *IEEE Transactions on Antennas and Propagation*, 2019, **67**, 2769-2774, doi: 10.1109/tap.2019.2897489.
[21] S. Modak, T. Khan, A slotted UWB-MIMO antenna with quadruple band-notch characteristics using mushroom EBG structure, *AEU - International Journal of Electronics and Communications*, 2021, **134**, 153673-153679, doi: 10.1016/j.aeue.2021.153673.
[22] S. R. Thummaluru, R. Kumar, R. K. Chaudhary, Isolation enhancement and radar cross section reduction of MIMO antenna with frequency selective surface, *IEEE Transactions on Antennas and Propagation*, 2018, **66**, 1595-1600, doi: 10.1109/tap.2018.2794417.
[23] T. Hassan, M. U. Khan, H. Attia, M. S. Sharawi, An FSS based correlation reduction technique for MIMO antennas, *IEEE Transactions on Antennas and Propagation*, 2018, **66**, 4900-4905, doi: 10.1109/tap.2018.2842256.
[24] A. A. Ibrahim, M. A. Abdalla, CRLH MIMO antenna with reversal configuration, *AEU - International Journal of Electronics and Communications*, 2016, **70**, 1134-1141, doi: 10.1016/j.aeue.2016.05.012.
[25] X. Zhao, S. P. Yeo, L. C. Ong, Planar UWB MIMO antenna with pattern diversity and isolation improvement for mobile platform based on the theory of characteristic modes, *IEEE Transactions on Antennas and Propagation*, 2017, **66**, 420-425, doi: 10.1109/TAP.2017.2768083.
[26] M. Li, L. Jiang, K. L. Yeung, A general and systematic method to design neutralization lines for isolation enhancement in MIMO antenna arrays, *IEEE Transactions on Vehicular Technology*, 2020, **69**, 6242-6253, doi: 10.1109/TVT.2020.2984044.
[27] S. Wang, Z. Du, Decoupled Dual-Antenna System Using Crossed Neutralization Lines for LTE/WWAN Smartphone Applications, *IEEE Antennas and Wireless Propagation*, 2014, **14**, 523-526, doi: 10.1109/LAWP.2014.2371020.
[28] R. N. Tiwari, P. Singh, B. K. Kanaujia, K. Srivastava, Neutralization technique based two and four port high isolation MIMO antennas for UWB communication, *AEU - International Journal of Electronics and Communications*, 2019, **110**, 152828, doi: 10.1016/j.aeue.2019.152828.
[29] D. Gao, Z.-X. Cao, S.-D. Fu, X. Quan, P. Chen, A novel slot-array defected ground structure for decoupling microstrip antenna array, *IEEE Transactions on Antennas and Propagation*, 2020, **68**, 7027-7038, doi: 10.1109/tap.2020.2992881.
[30] M. Irshad Khan, M. I. Khattak, S. U. Rahman, A. B. Qazi, A. A. Telba, A. Sebak, Design and investigation of modern UWB-MIMO antenna with optimized isolation, *Micromachines*, 2020, **11**, 432, doi: 10.3390/mi11040432.
[31] W. Yin, S. Chen, J. Chang, C. Li, S. K. Khamas, CPW fed compact UWB 4-element MIMO antenna with high isolation, *Sensors*, 2021, 21, 2688, doi: 10.3390/s21082688.
[32] M. S. Sharawi, A. T. Hassan, M. U. Khan, Correlation coefficient calculations for MIMO antenna systems: A comparative study, *International Journal of Microwave and Wireless Technologies*, 2017, **9**, 1991-2004, doi: 10.1017/S1759078717000903.
[33] S. H. Chae, S.-K. Oh, S.-O. Park, Analysis of mutual coupling, correlations, and TARC in WiBro MIMO array antenna, *IEEE Antennas and Wireless Propagation Letters*, 2007, **6**, 122-125, doi: 10.1109/lawp.2007.893109.
[34] A. Alayón Glazunov, A. F. Molisch, F. Tufvesson, Mean effective gain of antennas in a wireless channel, *IET Microwaves, Antennas & Propagation*, 2009, **3**, 214, doi: 10.1049/iet-map: 20080041.
[35] S. Ullah, C. Ruan, M. S. Sadiq, T. U. Haq, A. K. Fahad, W.

He, Super wide band, defected ground structure (DGS), and stepped meander line antenna for WLAN/ISM/WiMAX/UWB and other wireless communication applications, *Sensors*, 2020, 20, 1735, doi: 10.3390/s20061735.
[36] J. Zhu, S. Li, B. Feng, L. Deng, S. Yin, Compact dual-polarized UWB quasi-self-complementary MIMO/diversity antenna with band-rejection capability, *IEEE Antennas and Wireless Propagation Letters*, 2016, **15**, 905-908, doi: 10.1109/lawp.2015.2479622.
[37] A. Iqbal, O. A. Saraereh, A. W. Ahmad, S. Bashir, Mutual coupling reduction using F-shaped stubs in UWB-MIMO antenna, *IEEE Access*, 2018, **6**, 2755-2759, doi: 10.1109/access.2017.2785232.
[38] G. Srivastava, A. Mohan, Compact MIMO slot antenna for UWB applications, *IEEE Antennas and Wireless Propagation Letters*, 2016, **15**, 1057-1060, doi: 10.1109/lawp.2015.2491968.

Author Information

Praveen Kumar *received the B.E. degree in electronics and communication engineering and the M.Tech. degree in microelectronics and control systems from Visvesvaraya Technological University, Belagavi, Karnataka, India. He is currently pursuing the Ph.D. degree with the Department of Electronics and Communication Engineering, Manipal Institute of Technology, Manipal Academy of Higher Education, Manipal, India. His research interests include microstrip antennas. He is a Member of IETE, India.*

Tanweer Ali *(Senior Member, IEEE) is currently working as an Assistant Professor-Senior Scale with the Department of Electronics and Communication Engineering, Manipal Institute of Technology, Manipal Academy of Higher Education, Manipal. He is an active researcher in the field of microstrip antennas, wireless communication, and microwave imaging. He has been listed in top 2% researcher across the world recently by the prestigious list published by Stanford University, USA indexed by Scopus. He has published more than 115 papers in reputed web of science (SCI) and scopus indexed journal and conferences and also has filled two Indian patents. He has more than 1000 citations with an h-index of 19 and i-10 index of 28. Presently he is guiding 4 regular PhD students and 5 part-time PhD students and is heading the antenna research group at MIT, Manipal. In 2020 he has received best Ph.D. thesis award from Board of IT Education (BITES), Karnataka. He is on the board of reviewers of journals, like the IEEE TRANSACTIONS ON ANTENNAS AND PROPAGATION, IEEE ANTENNAS AND WIRELESS PROPAGATION LETTERS, IEEE ACCESS, IET Microwaves, Antennas and Propagation, Electronics Letter (IET), Wireless Personal Communications (WPCs) (Springer), AEU-International Journal of Electronics and Communications, Microwave and Optical Technology Letters (MOTL) (Wiley), International Journal of Antennas and Propagation (Hindawi), Advanced Electromagnetics, Progress in Electromagnetics Research (PIER), KSII Transactions on Engineering Science, International Journal of Microwave and Wireless Technologies, Frequencez, Radioengineering, IEEE open Journal of Antennas and Propagation and many more.*

Manohara Pai M. M. *received the Ph.D. degree in computer science and engineering from the Department of Information and Communication Technology, Manipal Institute of Technology, Manipal Academy of Higher Education, Manipal, India, where he has been a Professor, for the last 27 years. He holds six patents to his credit and has published 80 articles in national and international journals/ conference proceedings. He has published two books and guided five Ph.D.'s and 65 master theses. His research interests include data analytics, cloud computing, the IoT, computer networks, mobile computing, scalable video coding, and robot motion planning. He is a Life Member of ISTE and a Life Member of Systems Society of India. He is also the Chair of the IEEE Mangalore SubSection, in 2019.*

